Supplementary methods and results for the paper: Measurement of individual color space using luminous vector field

David Alleysson[1] **and David Méary**[1]

[1] *Univ. Grenoble Alpes, Univ. Savoie Mont Blanc, CNRS, LPNC, 38000 Grenoble, France*
[*] *Corresponding author: David.Alleysson (at) univ-grenoble-alpes.fr*

Compiled February 1, 2023

http://dx.doi.org/10.1364/ao.XX.XXXXXX

S1. SUPPLEMENTARY METHOD

SA. Display calibration

The general model of display calibration is shown in Figure S1. We measure the spectral emission of the screen with the Konika-Minolta CS2000 which returns spectral values in Watt in the range $[\lambda_m = 380, \lambda_M = 780]$ with a step of 1nm. We convert these values into 1/683 Watt by multiplying by 683. This allows luminance calculation in candela per meter square as a direct scalar product between a light spectrum and $V(\lambda)$, without normalisation constant. Fifty-two levels of digital values ranging from 0 to 1 with a step of 5/255 are measured for the colors red (R), green (G), blue (B), gray (R+G+B), yellow (R+G), magenta (R+B) and cyan (G+B). We use only the RGB data to define the model and verify with the other data (Cyan, Magenta, Yellow, Gray) that the model is accurate enough to predict any radiance spectrum $|m\rangle$ produced by the screen. The model writes:

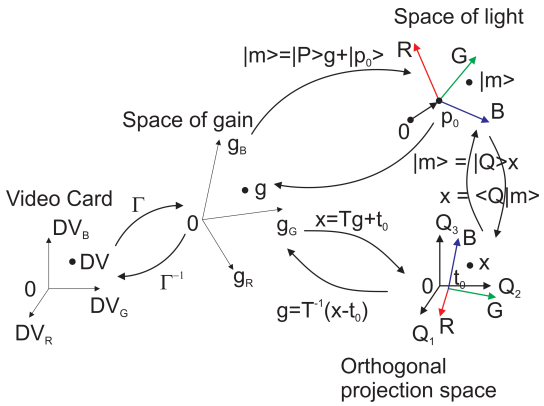

Fig. S1. Display calibration. This calibration is meant to create a three-dimensional Euclidean space which serves as the basis for determining the radiance of light functions emitted from the screen. We associate to the triplet of digital values DV a triplet of gain via a reversible nonlinear function Γ. From the vector of gain, we predict the spectral radiance of the light produced by the display. We map orthogonal functions $Q_1Q_2Q_3$ to the RGB primaries of the display. A direct conversion from the orthogonal space to the space of gains is set up which allows through Γ^{-1} to find numerical DV values corresponding to any point in the orthogonal space $Q_1Q_2Q_3$.

$$|m\rangle = |P\rangle g + |p_0\rangle \quad \textbf{(S1)}$$

The matrix $|P\rangle = [|R\rangle, |G\rangle, |B\rangle]$ is a $N \times 3$ ($N = 401$) matrix containing the prototypical functions $|R\rangle$, $|G\rangle$ and $|B\rangle$ of the screen phosphor, corresponding to the emission spectra for $DV = (1,0,0)$, $DV = (0,1,0)$ and $DV = (0,0,1)$. The vector $|p_0\rangle$ is the black level of the screen, i.e. the spectral emission for $DV = (0,0,0)$. The vector g contains the gain value per channel (between 0 and 1) that weights the prototypical functions according to $g = \Gamma(DV)$, where $DV = (DV_R, DV_G, DV_B)$ is a vector that represents the digital values for the RGB channels. The vector function Γ is a piecewise nonlinear vector function of DV defined by :

$$\Gamma\colon DV \in [0,1]^3 \to g \in [0,1]^3$$

$$DV \mapsto g = \Gamma(DV) = \begin{bmatrix} \Gamma_R(DV_R) \\ \Gamma_G(DV_G) \\ \Gamma_B(DV_B) \end{bmatrix} \quad \textbf{(S2)}$$

$$\Gamma_c(DV_c) = \{a_{c,i} + b_{c,i} x^{\gamma_{c,i}}, x_{c,i-1} \le x \le x_{c,i}\}_{i=1..M}$$
$$c \in \{R,G,B\},\ a_{c,1} = 0,\ b_{c,M} = 1,\ x_{c,0} = 0,\ x_{c,M} = 1$$

We use $M = 5$ branches for piecewise Γ functions. By constraining the branches to connect at the point $x_{c,i}$ and having a right derivative equal to the left derivative at the branch connection points, the parameters $a_{c,i}$ and $b_{c,i}$ are constrained. We use nonlinear least squares estimation to compute the other four parameters $x_{c,i}$ and the five parameters $\gamma_{c,i}$ for each color channel c, resulting in three times nine parameters. The prototype phosphor

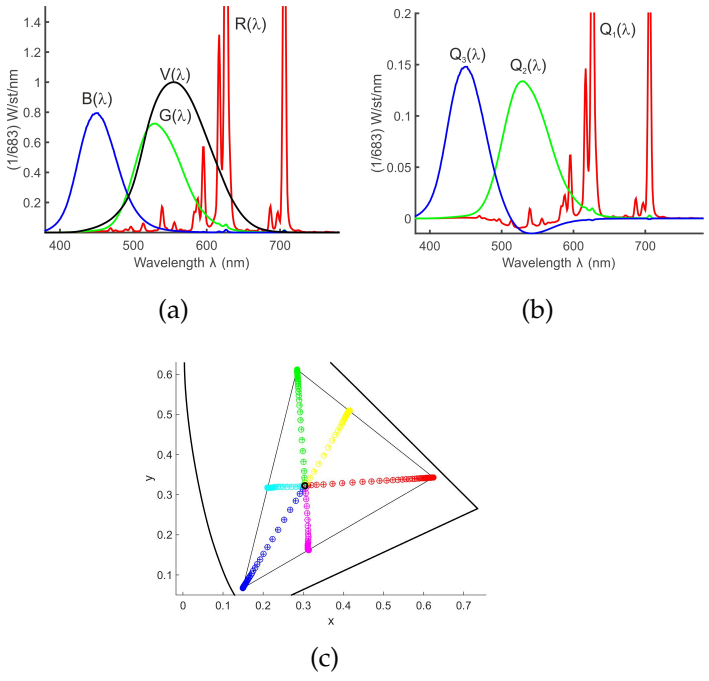

Fig. S2. Euclidean model of the display. (a) Measured emission spectra for the three phosphors of the display expressed in $(1/683)$ Watt, along with relative spectral efficiency of the eye $V(\lambda)$. (b) Associated orthogonal functions $Q_i(\lambda)$. (c) Evaluation of the model in CIE1931-xy chromaticity diagram. Crosses are measured values and circles are model predictions; they overlap.

functions included in the $|P\rangle$ matrix are not orthogonal functions for the scalar product defined in Equation (4). Contrary to what is described in Equation (5), we use Gram-Schmidt orthogonalization on Matlab [2] to derive the orthogonal functions $|Q\rangle = [|Q_1\rangle\ |Q_2\rangle\ |Q_3\rangle]$ from $|P\rangle$. For convenience, we impose $|Q_2\rangle$ to be collinear with the phosphor $|G\rangle$. The transformation of the functions $|P\rangle$ into functions $|Q\rangle$ is given by the 3×3 matrix $T = \langle Q|P\rangle$ with $|Q\rangle = |P\rangle T^{-1}$.

According to the equation S1, the light spectrum $|m\rangle$ emitted by the computer screen corresponds to the point $x = \langle Q|m\rangle = Tg + t_0$ with $t_0 = \langle Q|p_0\rangle$ in the system of coordinates spanned by $|Q\rangle$, isomorphic to $\mathbb{R}^3$. Conversely, for a point x in the color space of the screen, we can calculate the corresponding numerical value by $DV = \Gamma^{-1}(T^{-1}(x - t_0))$.

Figure S2 shows the measured functions $|P\rangle$, the orthogonal primaries $|Q\rangle$ and the evaluation of the screen model in the CIE1931-xy chromaticity diagram.

SB. Adaptive procedure for estimating the angle of the subjective assessment of no motion

The goal of the modified minimum motion experiment is to measure the angle at which the stimulus no longer produces a reliable perception of leftward or rightward motion. The point of subjective evaluation of minimum motion can only be determined statistically. We set-up an adaptive procedure for estimating the angle of minimum motion. We fixed the number of trial in a particular condition (chosen point and plane) to thirty trials. We used vector V_λ and its projection onto planes P_1 and P_2 as a prior for angle estimation which corresponds to observer angle equal to zero relative to $V(\lambda)$.

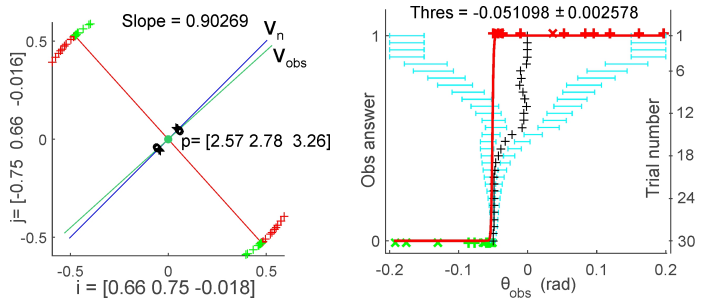

Fig. S3. Adaptive procedure for minimum motion angle estimation. (a) Representation of trials and observer's response in plane P_2 with coordinate system (p, i, j). The green and red markers represent the observer responses, right or left depending on the sign of the variable d coding for motion direction in the equation of the stimulus (See article section 3B). The green line indicates the estimated direction of the luminous vector. The blue line indicates the direction of the projection of V_λ (or equivalently its normalized version v_n) in the plane P_2. (b) The progression of intervals of draw along trials (cyan segments) and the adaptive procedure. The green and red markers corresponds to those in figure (a). The two types of crosses $+$ and $\times$ correspond to $d = 1$ and $d = -1$. Black crosses represent the current estimate of μ along trials.

The Figure S3(a) shows a typical minimum motion session in the P_2 plane. The Figure S3(b) shows the session in

the angle-response diagram. We begin the experiment by choosing the first four trials randomly in two fixed intervals far away from angle zero to ensure that the observer will see motion. This also fixes the interval in which the subjective assessment of the angle falls. The adaptive procedure begins after the first four trials. The set of available responses $(\theta, resp)$ where θ is the test angle and $resp \in [0,1]$ is the observer's response (left is zero and right is one if the direction of the stimulus is $d = 1$, and the reverse if $d = -1$, see section 3B for definition of d) used to determine a fit by a sigmoid psychometric function of the type $resp = 1/(1 + e^{-(\theta-\mu)/\sigma})$ using lsqcurvefit in @MATLAB (μ is the current estimate of the angle). Current estimate along trials of θ is shown by black cross and psychometric fit by red curve in Figure S3(b).

The size of the draw intervals is driven by σ which is the variance parameter in the psychometric function. The position of the intervals is proportionally moved closer together until they touch for the last thirtieth trial. The trial angle is chosen in the left or right interval based on the past number of trials to the left or right to adjust the number of trials below or above the current estimate of μ. On the thirtieth trial, the angle of subjective equality is given by the parameter μ in the psychometric function above.

SC. Estimation of observer's parameters A and a_0

Measurements for one observer result in two matrices X and V of size $3 \times N$ containing coordinates of the different points p and the corresponding vector coordinates v for the N color points p.

SC.1. Affine model $V = 2AX + x_0$

The affine model is calculated by first adding a homogeneous variable equal to one per point and vector. We call those matrix $\overline{X}$ and $\overline{V}$ given by:

$$\overline{X} = \begin{bmatrix} p_{11} & \dots & p_{1N} \\ p_{21} & \dots & p_{2N} \\ p_{31} & \dots & p_{3N} \\ 1 & \dots & 1 \end{bmatrix} \quad \overline{V} = \begin{bmatrix} v_{11} & \dots & v_{1N} \\ v_{21} & \dots & v_{2N} \\ v_{31} & \dots & v_{3N} \\ 1 & \dots & 1 \end{bmatrix} \tag{S3}$$

Affine model $\overline{V} = M\overline{X}$ is given for:

$$M = \overline{V}\overline{X}^t \left(\overline{X}\overline{X}^t\right)^{-1} = \begin{bmatrix} & 2B & & a_0 \\ & & & \\ 0 & 0 & 0 & 1 \end{bmatrix} \tag{S4}$$

The vector field estimated by the model is given by $\widetilde{\overline{V}} = M\overline{X}$ or equivalently $\widetilde{V} = 2BX + a_0$ by removing the homogeneous variable. The resulting matrix B is non-symmetric because we did not choose the points p around the symmetry axis of the metric which was unknown. A symmetric matrix can be obtained by considering the matrix $A = (B + B^t)/2$. The matrix A is not a model for the vector field but produces the same surface as the matrix B [1].

The mean square error displayed in Table 1 is given by the mean square error $\text{mse}_1 = E\left\{\left\|\widetilde{V} - V\right\|^2\right\}$.

SC.2. Linear model $V = 2AX$

We test the second model $V = 2AX$ without the shift in origin. We compute the matrix A by the pseudo inverse, $A = VX^t(XX^t)^{-1}/2$. Estimated vectors by the model are given by $\overline{V} = 2AX$. Mean square error is calculated as $\text{mse}_2 = E\left\{\left\|\widetilde{V} - V\right\|^2\right\}$.

SC.3. Constant model $V = ra_0$

The third model is a constant model calculated as the average of vectors divided by the radius of the sphere, $a_0 = E\{V/r\}$. Estimated vectors by the model is $\overline{V} = ra_0$. Mean square error is calculated as $\text{mse}_3 = E\left\{\left\|\widetilde{V} - V\right\|^2\right\}$.

We have tested the three alternative models for predicting V from X. Comparing the three models using paired samples t-test we found that the mean mse over subject for the affine model (M=1.08E-6; SD=1.36E-6) was smaller than that of the linear model (M=1.86E-6; SD=1.96E-6); [$t(23)$ = -4.6, $p < 0.001$]. The linear model was also better than the constant model (M=18.86E-6; SD=18.7E-6); [$t(23)$ = -4.58, $p < 0.001$]. Consequentially, the affine model is also better than the constant model.

SD. Surface from orthogonal vector field

The general equation of a quadratic surface $f(x_1, x_2, x_3)$ in $\mathbb{R}^3$ is given by the set of points of coordinates $x = (x_1, x_2, x_3)$ such that:

$$\begin{aligned} f(x_1, x_2, x_3) = {} & ax_1^2 + bx_2^2 + cx_3^2 + 2dx_2x_3 + 2ex_1x_3 \\ & + 2fx_1x_2 + gx_1 + hx_2 + ix_3 - j = 0 \end{aligned} \tag{S5}$$

which writes in matrix-vector form:

$$\begin{aligned} & \begin{bmatrix} x_1 & x_2 & x_3 \end{bmatrix} \underbrace{\begin{bmatrix} a & f & e \\ f & b & d \\ e & d & c \end{bmatrix}}_{A} \begin{bmatrix} x_1 \\ x_2 \\ x_3 \end{bmatrix} \\ & \quad + \begin{bmatrix} x_1 & x_2 & x_3 \end{bmatrix} \underbrace{\begin{bmatrix} g \\ h \\ i \end{bmatrix}}_{a_0} - j = 0 \\ & \Leftrightarrow x^t A x + x^t a_0 - j = 0 \end{aligned} \tag{S6}$$

Coordinates of orthogonal vectors to any point of coordinates $x = (x_1, x_2, x_3)$ of the surface are given by the gradient of $f(x_1, x_2, x_3)$ which from Equation S5 writes:

$$\begin{aligned}\nabla f(x_1,x_2,x_3) &= \begin{bmatrix} \frac{\partial f(x_1,x_2,x_3)}{\partial x_1} \\ \frac{\partial f(x_1,x_2,x_3)}{\partial x_2} \\ \frac{\partial f(x_1,x_2,x_3)}{\partial x_3} \end{bmatrix} \\ &= 2\begin{bmatrix} ax_1 + fx_2 + ex_3 \\ fx_1 + bx_2 + dx_3 \\ ex_1 + dx_2 + cx_3 \end{bmatrix} + \begin{bmatrix} g \\ h \\ i \end{bmatrix} \\ &= 2Ax + a_0 \end{aligned} \quad \textbf{(S7)}$$

Thus, from the affine model of the orthogonal vector field, $v = 2Ax + a_0$, the surface is completely defined by $x^t Ax + x^t a_0 = j$.

S2. SUPPLEMENTARY RESULTS

SA. Supplementary results on Weber ratio

Weber ratios are calculated along each projective line by the ratio between the norm of the luminous vector $\|v_{obs}\|$ at a point p of coordinate x divided by the radius r of the sphere on which the point is taken (or equivalently the Euclidean norm of x, $\|x|$), $WR(r) = \|v_{obs}\|/r$. As shown in Figure S4, the Weber ratio changes with the color of the projective line.

Corrected Weber ratios are calculated using the hyperbolic norm of the point p, $|x| = \sqrt{(x - x_0)^t H (x - x_0)}$, with x_0 and H are the observer's hyperbolic model, by the following equation:

$$WR_c(r) = \mu \frac{WR(r)}{aE_r\{|x|\} + b} \quad \textbf{(S8)}$$

where $E_r\{|x|\}$ is the average over the radius r of the hyperbolic norm of x. a and b are the parameters of the order one polynomial fit between average Weber ratio and average hyperbolic norm of x across radius. And μ is a factor for having the same average for Weber ratio and corrected Weber ratio. The corrected Weber ratio has a lower standard deviation along the different colors than the Weber ratio.

We compute the average ratio along projective lines between the standard deviation of the Weber ratio and the standard deviation of the corrected Weber ratio. This ratio is called f. This can be understood as a factor of consistency of the corrected Weber ratio along projective lines. A larger factor of consistency f means that the correction with hyperbolic norm had better improved the consistency of the corrected Weber ratio along colors. The table S1 shows the factor of consistency for all observers along with their estimated parameters.

In column five of Table S1 it is shown that corrected Weber ratios are more consistent for all observers since the value is always greater than one. The average consistency factor is 3.54 which supports the idea that the hyperbolic

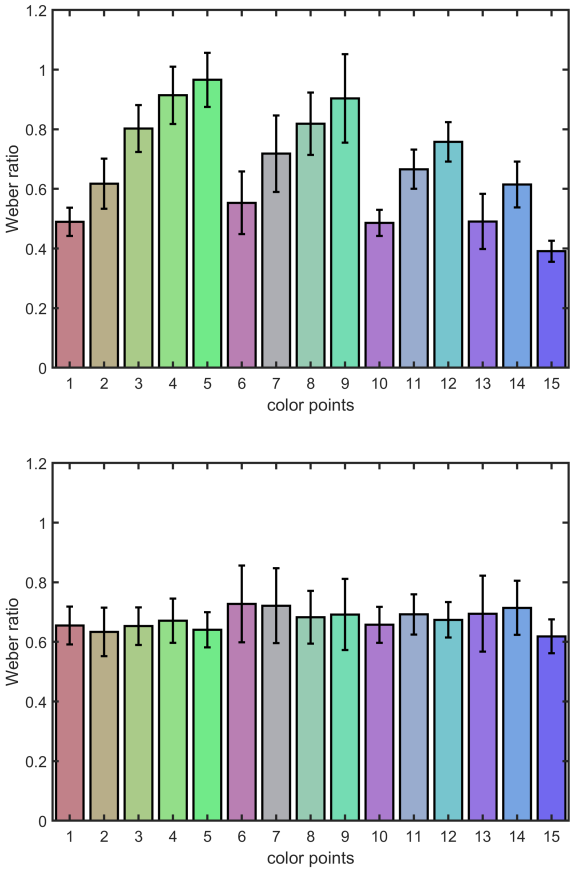

Fig. S4. Change of the Weber ratio with the color of the projective line. Top: Weber ratio is estimated for each projective line as the norm of the luminous vector divided by the radius of the sphere on which the corresponding point is taken. Depending on the color of the projective line, the Weber ratio changes. Bottom: Corrected Weber ratio by the hyperbolic norm.

Table S1. Parameters for correction (μ, a, b) and consistency f

Obs	μ	a	b	f	Obs	μ	a	b	f
1	0.77	12.78	0.38	1.70	13	0.83	14.34	0.43	4.47
2	0.59	12.82	0.28	3.21	14	0.50	12.03	0.14	2.04
3	0.27	18.97	0.16	3.07	15	0.34	15.69	0.20	3.47
4	0.41	15.22	0.28	4.62	16	0.81	13.30	0.32	4.27
5	0.55	11.39	0.24	2.68	17	0.92	17.94	0.61	3.86
6	0.90	12.10	0.47	3.57	18	0.30	16.24	0.17	2.62
7	1.20	10.52	0.36	5.15	19	0.58	16.36	0.31	4.78
8	0.50	13.35	0.13	3.99	20	0.47	10.62	0.23	2.10
9	0.69	11.74	0.19	3.06	21	0.42	13.27	0.17	3.76
10	1.43	12.97	0.66	5.86	22	0.42	17.00	0.31	1.79
11	0.95	16.80	0.51	3.61	23	0.55	13.51	0.21	1.64
12	0.89	12.98	0.33	3.33	24	0.37	15.10	0.20	6.25

norm of the point $|x|$ can regulate Weber's law across projection lines.

REFERENCES

1. Csaki, F. (1970). A concise proof of Sylvester's theorem. Periodica Polytechnica Electrical Engineering, 14(2), 105-112.
2. Ahmadzadeh, R.(2022). Stabilized Gram-Schmidt Orthonormal Method, MATLAB Central File Exchange. Retrieved April 14, 2022.